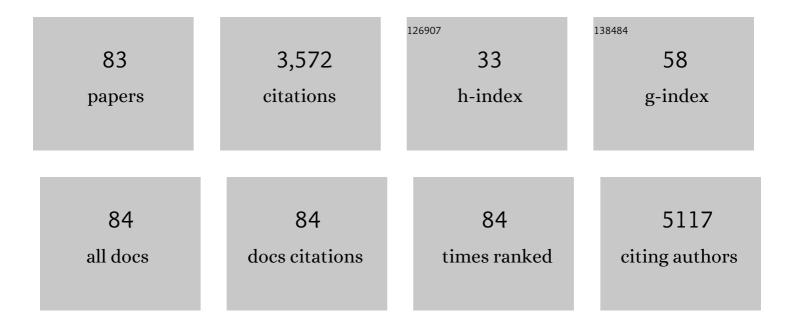
## **Thomas Feurer**

List of Publications by Year in descending order

Source: https://exaly.com/author-pdf/2529173/publications.pdf Version: 2024-02-01



#	Article	IF	CITATIONS
1	Low-temperature-processed efficient semi-transparent planar perovskite solar cells for bifacial and tandem applications. Nature Communications, 2015, 6, 8932.	12.8	398
2	Progress in thin film CIGS photovoltaics – Research and development, manufacturing, and applications. Progress in Photovoltaics: Research and Applications, 2017, 25, 645-667.	8.1	248
3	High-efficiency inverted semi-transparent planar perovskite solar cells in substrate configuration. Nature Energy, 2017, 2, .	39.5	247
4	Advanced Alkali Treatments for Highâ€Efficiency Cu(In,Ga)Se <sub>2</sub> Solar Cells on Flexible Substrates. Advanced Energy Materials, 2019, 9, 1900408.	19.5	175
5	High-Efficiency Polycrystalline Thin Film Tandem Solar Cells. Journal of Physical Chemistry Letters, 2015, 6, 2676-2681.	4.6	166
6	Terahertz near-field imaging of electric and magnetic resonances of a planar metamaterial. Optics Express, 2009, 17, 3826.	3.4	123
7	Lattice modes mediate radiative coupling in metamaterial arrays. Optics Express, 2009, 17, 22108.	3.4	105
8	Terahertz polariton propagation in patterned materials. Nature Materials, 2002, 1, 95-98.	27.5	95
9	Terahertz near-field microscopy of complementary planar metamaterials: Babinet's principle. Optics Express, 2011, 19, 2537.	3.4	88
10	High Aspect Ratio Plasmonic Nanostructures for Sensing Applications. ACS Nano, 2011, 5, 6374-6382.	14.6	80
11	Nanodoublers as deep imaging markers for multi-photon microscopy. Optics Express, 2009, 17, 15342.	3.4	71
12	Efficiency Improvement of Nearâ€Stoichiometric CuInSe <sub>2</sub> Solar Cells for Application in Tandem Devices. Advanced Energy Materials, 2019, 9, 1901428.	19.5	69
13	Flexible NIR-transparent perovskite solar cells for all-thin-film tandem photovoltaic devices. Journal of Materials Chemistry A, 2017, 5, 13639-13647.	10.3	68
14	Compositionally Graded Absorber for Efficient and Stable Nearâ€Infraredâ€Transparent Perovskite Solar Cells. Advanced Science, 2018, 5, 1700675.	11.2	65
15	Bulk and surface recombination properties in thin film semiconductors with different surface treatments from time-resolved photoluminescence measurements. Scientific Reports, 2019, 9, 5385.	3.3	65
16	Controlled growth of PbI <sub>2</sub> nanoplates for rapid preparation of CH <sub>3</sub> NH <sub>3</sub> PbI <sub>3</sub> in planar perovskite solar cells. Physica Status Solidi (A) Applications and Materials Science, 2015, 212, 2708-2717.	1.8	63
17	Nearâ€Infraredâ€Transparent Perovskite Solar Cells and Perovskiteâ€Based Tandem Photovoltaics. Small Methods, 2020, 4, 2000395.	8.6	63
18	Iterative Fourier transform algorithm for phase-only pulse shaping. Optics Express, 2001, 9, 191.	3.4	57

2

#	Article	IF	CITATIONS
19	Terahertz ptychography. Optics Letters, 2018, 43, 543.	3.3	57
20	Solutionâ€Processed Lowâ€Bandgap Culn(S,Se) <sub>2</sub> Absorbers for Highâ€Efficiency Singleâ€Junction and Monolithic Chalcopyriteâ€Perovskite Tandem Solar Cells. Advanced Energy Materials, 2018, 8, 1801254.	19.5	56
21	Bandgap of thin film solar cell absorbers: A comparison of various determination methods. Thin Solid Films, 2019, 669, 482-486.	1.8	56
22	Towards jitter-free ultrafast electron diffraction technology. Nature Photonics, 2020, 14, 245-249.	31.4	55
23	High-Mobility In <sub>2</sub> O <sub>3</sub> :H Electrodes for Four-Terminal Perovskite/CuInSe <sub>2</sub> Tandem Solar Cells. ACS Nano, 2020, 14, 7502-7512.	14.6	54
24	Single-graded CIGS with narrow bandgap for tandem solar cells. Science and Technology of Advanced Materials, 2018, 19, 263-270.	6.1	51
25	Refractive indices of layers and optical simulations of Cu(In,Ga)Se <sub>2</sub> solar cells. Science and Technology of Advanced Materials, 2018, 19, 396-410.	6.1	46
26	Five picocoulomb electron bunch generation by ultrafast laser-induced field emission from metallic nano-tip arrays. Applied Physics Letters, 2011, 99, .	3.3	40
27	Solvation-Driven Charge Transfer and Localization in Metal Complexes. Accounts of Chemical Research, 2015, 48, 1432-1440.	15.6	39
28	CNT-based bifacial perovskite solar cells toward highly efficient 4-terminal tandem photovoltaics. Energy and Environmental Science, 2022, 15, 1536-1544.	30.8	39
29	Second harmonic generation based on strong field enhancement in nanostructured THz materials. Optics Express, 2011, 19, 7262.	3.4	38
30	Dispersion control with reflection grisms of an ultra-broadband spectrum approaching a full octave. Optics Express, 2010, 18, 27900.	3.4	37
31	Cu(In,Ga)Se2 solar cells on low cost mild steel substrates. Solar Energy, 2018, 175, 25-30.	6.1	35
32	Tailored lead iodide growth for efficient flexible perovskite solar cells and thin-film tandem devices. NPG Asia Materials, 2018, 10, 1076-1085.	7.9	35
33	How band tail recombination influences the open ircuit voltage of solar cells. Progress in Photovoltaics: Research and Applications, 2022, 30, 702-712.	8.1	35
34	Ultra low-noise coherent supercontinuum amplification and compression below 100 fs in an all-fiber polarization-maintaining thulium fiber amplifier. Optics Express, 2019, 27, 35041.	3.4	34
35	THz generation by optical rectification of near-infrared laser pulses in the organic nonlinear optical crystal HMQ-TMS. Optical Materials Express, 2014, 4, 1586.	3.0	33
36	Disentangling size effects and spectral inhomogeneity in carbon nanodots by ultrafast dynamical hole-burning. Nanoscale, 2018, 10, 15317-15323.	5.6	33

#	Article	IF	CITATIONS
37	RbF post deposition treatment for narrow bandgap Cu(In,Ga)Se2 solar cells. Thin Solid Films, 2019, 670, 34-40.	1.8	33
38	Radially polarized mode-locked Nd:YAG laser. Optics Letters, 2009, 34, 2030.	3.3	32
39	Impact of compositional grading and overall Cu deficiency on the near-infrared response in Cu(In,) Tj ETQq1 1 0	.784314 rg 8.1	gBT <sub>3/2</sub> Overlock
40	Monolithic CIGS–Perovskite Tandem Cell for Optimal Light Harvesting without Current Matching. ACS Photonics, 2017, 4, 861-867.	6.6	27
41	Improved retrieval of complex supercontinuum pulses from XFROG traces using a ptychographic algorithm. Optics Letters, 2016, 41, 4903.	3.3	25
42	Revealing the perovskite formation kinetics during chemical vapour deposition. Journal of Materials Chemistry A, 2020, 8, 21973-21982.	10.3	24
43	Understanding optimal control results by reducing the complexity. Chemical Physics, 2005, 318, 207-216.	1.9	21
44	Graphene Metamaterials for Intense, Tunable, and Compact Extreme Ultraviolet and Xâ€Ray Sources. Advanced Science, 2020, 7, 1901609.	11.2	21
45	A MS-CASPT2 study of the low-lying electronic excited states of CH2BrCl. Chemical Physics Letters, 2001, 350, 155-164.	2.6	19
46	Near-field investigation of induced transparency in similarly oriented double split-ring resonators. Optics Letters, 2011, 36, 1683.	3.3	19
47	Superbroadband fluorescence fiber fabricated with granulated oxides. Optics Letters, 2008, 33, 1050.	3.3	18
48	Surface Passivation for Reliable Measurement of Bulk Electronic Properties of Heterojunction Devices. Small, 2016, 12, 5339-5346.	10.0	17
49	Temporal fine structure of all-normal dispersion fiber supercontinuum pulses caused by non-ideal pump pulse shapes. Optics Express, 2020, 28, 16579.	3.4	17
50	3D-printed THz wave- and phaseplates. Optics Express, 2021, 29, 27160.	3.4	16
51	Direct visualization of phonon-polariton focusing and amplitude enhancement. Journal of Chemical Physics, 2002, 117, 2897-2901.	3.0	14
52	THz near-field enhancement by means of isolated dipolar antennas: the effect of finite sample size. Optics Express, 2016, 24, 4552.	3.4	14
53	Novel back contact reflector for high efficiency and doubleâ€graded Cu(In,Ga)Se <sub>2</sub> thinâ€film solar cells. Progress in Photovoltaics: Research and Applications, 2018, 26, 894-900.	8.1	14
54	Dipole Moment and Polarizability of Tunable Intramolecular Charge Transfer States in Heterocyclic Ï€-Conjugated Molecular Dyads Determined by Computational and Stark Spectroscopic Study. Journal of Physical Chemistry C, 2018, 122, 9346-9355.	3.1	13

#	Article	IF	CITATIONS
55	All-fiber frequency-stabilized erbium doped ring laser. Optics Express, 2010, 18, 26821.	3.4	12
56	Precise Se-flux control and its effect on Cu(In,Ca)Se 2 absorber layer deposited at low substrate temperature by multi stage co-evaporation. Thin Solid Films, 2017, 633, 18-22.	1.8	12
57	Chromium nitride as a stable cathode current collector for all-solid-state thin film Li-ion batteries. RSC Advances, 2017, 7, 26960-26967.	3.6	11
58	Photocycle of Excitons in Nitrogen-Rich Carbon Nanodots: Implications for Photocatalysis and Photovoltaics. ACS Applied Nano Materials, 2020, 3, 6925-6934.	5.0	11
59	Skirting terahertz waves in a photo-excited nanoslit structure. Applied Physics Letters, 2014, 104, .	3.3	10
60	Tunable Lifetimes of Intramolecular Charge-Separated States in Molecular Donor–Acceptor Dyads. Journal of Physical Chemistry C, 2019, 123, 8500-8511.	3.1	9
61	Extending time-domain ptychography to generalized phase-only transfer functions. Optics Letters, 2020, 45, 300.	3.3	9
62	Comparative theoretical analysis of continuous wave laser cutting of metals at 1 and 10Âμm wavelength. Applied Physics A: Materials Science and Processing, 2014, 116, 1353-1364.	2.3	8
63	Anti-Kasha Conformational Photoisomerization of a Heteroleptic Dithiolene Metal Complex Revealed by Ultrafast Spectroscopy. Journal of Physical Chemistry A, 2020, 124, 10687-10693.	2.5	8
64	Pulsed erbium fiber laser with an acetylene-filled photonic crystal fiber for saturable absorption. Optics Letters, 2011, 36, 3569.	3.3	7
65	Pulse-shaping assisted multidimensional coherent electronic spectroscopy. Journal of Chemical Physics, 2015, 142, 212451.	3.0	7
66	DNA-organized artificial LHCs – testing the limits of chromophore segmentation. Organic and Biomolecular Chemistry, 2020, 18, 6818-6822.	2.8	7
67	Application of nonreflecting boundary condition for numerical simulation of molecular photoionization dynamics. Journal of Applied Physics, 2000, 88, 2936-2942.	2.5	6
68	Influence of finite spatial resolution on single- and double-pass femtosecond pulse shapers. Optics Letters, 2010, 35, 4072.	3.3	6
69	Optically Controlled Electron Transfer in a Re <sup>I</sup> Complex. Chemistry - A European Journal, 2021, 27, 5399-5403.	3.3	6
70	ALD-ZnMgO and absorber surface modifications to substitute CdS buffer layers in co-evaporated CIGSe solar cells. EPJ Photovoltaics, 2020, 11, 12.	1.6	6
71	Optimization-Based Terahertz Imaging. IEEE Transactions on Terahertz Science and Technology, 2012, 2, 493-503.	3.1	5
72	Self-photopumped x-ray lasers from elements in the Ne-like and Ni-like ionization state. Optics Communications, 2017, 382, 288-293.	2.1	5

#	Article	IF	CITATIONS
73	Ultrashort pulse formation from a thulium-doped fiber laser: Self-characterization and mapping. Optics Communications, 2021, 486, 126747.	2.1	5
74	Inverse-Designed Narrowband THz Radiator for Ultrarelativistic Electrons. ACS Photonics, 2022, 9, 1143-1149.	6.6	5
75	THz Switching and THz Nonlinear Spectroscopy Applications. Chimia, 2011, 65, 316.	0.6	4
76	Spatiotemporal Visualization of THz Near-Fields in Metamaterial Arrays. Journal of Infrared, Millimeter, and Terahertz Waves, 2011, 32, 570-579.	2.2	4
77	Attoclock Ptychography. Applied Sciences (Switzerland), 2018, 8, 1039.	2.5	4
78	DNAâ€Organized Lightâ€Harvesting Antennae: Energy Transfer in Polyaromatic Stacks Proceeds through Interposed Nucleobase Pairs. Helvetica Chimica Acta, 2019, 102, e1900148.	1.6	4
79	Terahertz Selective Emission Enhancement from a Metasurface-Coupled Photoconductive Emitter in Quasi-Near-Field Zone. Plasmonics, 2020, 15, 263-269.	3.4	3
80	Optical Fibers With a Finite Metallic Core. Journal of Lightwave Technology, 2009, 27, 1454-1460.	4.6	2
81	Dispersion control with reflection grisms of an ultra-broadband spectrum approaching a full octave: erratum. Optics Express, 2011, 19, 12634.	3.4	0
82	National Center of Competence in Research: molecular ultrafast science and technology. Chimia, 2011, 65, 292-3.	0.6	0
83	High-resolution phase-sensitive sum frequency generation spectroscopy by time-domain ptychography.	3.3	Ο